NLDI GUIDANCE CONTROL LAWS
FOR CLOSE FORMATION FLIGHT

Giampiero Campa^, Brad Seanor^, Yu Gu^, Marcello R. Napolitano@

Department of Mechanical and Aerospace Engineering, West Virginia University, Morgantown, WV 26506/6106,

Abstract

This paper presents identification, control synthesis and simulation results for an YF-22 aircraft model designed, built, and instrumented at West Virginia University. The goal of the project was the experimental demonstration of formation flight for a set of 3 of the above models. In the planned flight configuration, a pilot on the ground maintained controls of the leader aircraft while a follower aircraft was required to maintain a pre-defined position and orientation with respect to the leader. In this paper, the identification of both a linear model and a nonlinear model of the aircraft from flight data is shown first. Then, the control laws, that feature a linear inner loop controller and a NLDI (nonlinear dynamic inversion) based outer loop guidance controller, are discussed in detail. Finally, both simulation and flight test results are presented.

1   Introduction

Autonomous formation flight is an important research area in the aerospace community. The investigation of control issues related to a leader-follower formation has lead to the introduction of different types of compensation-type controllers [1]. In Ref. [2] a formation flight control scheme was proposed based on the concept of Formation Geometry Center, also known as the Formation Virtual Leader. This paper presents design and results of a formation control project performed on a set of 3 YF-22 aircraft models that were designed, built, and instrumented at West Virginia University (WVU). One of the 3 WVU YF-22 models is shown in Figure 1. The model features an 3 m fuselage length with a 2 m wingspan for an approximate take-off weight of 23 Kg, including a 5 Kg electronic payload consisting on a PC-104 flight computer, a complete set of sensors, a GPS receiver and a set of RF modems used for data transmission.

Due to the limitations on the flight range, the WVU YF-22 models were expected to perform fairly tight maneuvers at high Euler angles and moderately high angular rates. Therefore, a specific issue in the design of a control scheme was to allow for formation control under these flight conditions. Another objective was to limit the amount of information exchange (between leader and follower) needed to maintain the predefined formation geometry.

Figure 1 - WVU YF-22 aircraft model

The paper is organized as follows. The second section describes the identification of a linear and nonlinear single aircraft model from collected flight data. The third section outlines the geometric characteristics of the formation. The fourth section outlines the design of the formation control laws. The final sections will present the simulation and visualization environments, together with the main formation flight experimental results. The symbols used throughout the paper are very standard, but readers less familiar with flight mechanics could consult [3] or download the FDC manual [4] as a reference.

2   System Identification of the WVU YF-22

Flight data for several maneuvers were collected for parameter identification purposes using the following on-board instrumentation:

- Absolute and differential pressure sensors: (SenSym ASCX15AN and SenSym ASCX01DN), used to calculate H and V (altitude and speed).
- Inertial Measurement Unit (Crossbow IMU-400) to measure Ax, Ay, Az, p, q, r, (accelerations, roll pitch and yaw rates).
- Vertical Gyro (Goodrich Sensor System VG34) to measure φ, θ, (roll and pitch angles).
- Nose probe (Space Age) to measure α and β (attack and sideslip angles).
- Potentiometers on the control surfaces to measure δ_E, δ_A, δ_R (elevators, ailerons and rudders deflections).

@ Professor, ^ Research Assistant Professor

Turn maneuvers, plus doublets on each control surface, were performed during the flights. A PC-104 based on-board computer collected in real time (at a rate of 100Hz) all of the above signals using the integrated data acquisition card (Diamond MM 32). The data were stored on a flash-card for post-flight downloading. A set of flight data was selected for the actual parameter estimation process, while a second set of data was selected for validation purposes.

2.1 Linear Model Identification

The linear model identification was performed with a 3-step process. First, the flight data time histories were smoothed and rearranged using simulink-based filters. Next, a batch Matlab file performed the actual identification algorithm. The last step of the model identification process was the validation of the linear model using time histories of the control surface deflections from the validation flight data. In other words, the simulated and true responses to the time histories of the control surface deflections (in the validation data set) were compared. Following the identification study, the estimated linear lateral-directional aerodynamic model was given by:

$$\begin{bmatrix} \dot{\beta} \\ \dot{p} \\ \dot{r} \\ \dot{\phi} \end{bmatrix} = \begin{bmatrix} 0.4299 & 0.0938 & -1.0300 & 0.2366 \\ -67.3341 & -7.9485 & 5.6402 & 0 \\ 20.5333 & -0.6553 & -1.9955 & 0 \\ 0 & 1 & 0 & 0 \end{bmatrix} \begin{bmatrix} \beta \\ p \\ r \\ \phi \end{bmatrix}$$
$$+ \begin{bmatrix} 0.2724 & -0.7713 \\ -101.8446 & 33.4738 \\ -6.2609 & -24.3627 \\ 0 & 0 \end{bmatrix} \begin{bmatrix} \delta_A \\ \delta_R \end{bmatrix} \quad (1)$$

The estimated longitudinal model was given by:

$$\begin{bmatrix} \dot{v} \\ \dot{\alpha} \\ \dot{q} \\ \dot{\theta} \end{bmatrix} = \begin{bmatrix} -0.2835 & -23.0959 & 0 & -0.1711 \\ 0 & -4.1172 & 0.7781 & 0 \\ 0 & -33.8836 & -3.5729 & 0 \\ 0 & 0 & 1 & 0 \end{bmatrix} \begin{bmatrix} v \\ \alpha \\ q \\ \theta \end{bmatrix}$$
$$+ \begin{bmatrix} 20.1681 \\ 0.5435 \\ -39.0847 \\ 0 \end{bmatrix} \delta_E \quad (2)$$

This model represents the aircraft in a steady and level flight at 42 m/s, 336m of altitude, with alpha and theta of 3 deg. This linear model was mainly used for control synthesis. For simulation purposes, a full nonlinear aircraft model was considered highly desirable if not necessary.

2.2 Nonlinear Model Identification

The identification of the mathematical model of a nonlinear system is a more challenging issue [5,6]. Most of the nonlinear identification efforts rely on both good physical insight [5] and some form of optimization algorithm like Steepest descent or Newton-Raphson [6]. The general nonlinear model of an aircraft system can be expressed (see for example [3]) as:

$$\dot{x} = f(x, \delta, G, F_A(x,\delta), M_A(x,\delta));$$
$$y = g(x, \delta, G, F_A(x,\delta), M_A(x,\delta)); \quad (3)$$

where x is the state vector (linear and angular positions and velocity), y is the output vector (linear and angular accelerations), δ is the input vector (surface deflections), G is a vector of geometric parameters and inertia coefficients, F_A and M_A are aerodynamic forces and moments acting on the aircraft; finally, f and g are the known analytic functions that express the dynamics and kinematics of a rigid body. The aerodynamic forces and moments are expressed using the aerodynamic coefficients C_D, C_Y, C_L, C_l, C_m, C_n :

$$F_A = \overline{q}S \begin{bmatrix} C_D(x,\delta) \\ C_Y(x,\delta) \\ C_L(x,\delta) \end{bmatrix}, M_A = \overline{q}S \begin{bmatrix} bC_l(x,\delta) \\ \overline{c}C_m(x,\delta) \\ bC_n(x,\delta) \end{bmatrix} \quad (4)$$

where S is the wing platform area, $\overline{q}$ the dynamic pressure, b the wingspan, and $\overline{c}$ the mean aerodynamic chord. The aerodynamic coefficients are often approximated by affine functions in x and δ; for example, for the lift coefficient:

$$C_L(x,\delta) = c_{L0} + c_{L\alpha}\alpha + c_{Lq}q + c_{L\delta_e}\delta_e \quad (5)$$

where, c_{L0} and the other three coefficients are usually called the "derivatives" of C_L.

Under the above assumptions, the nonlinear aircraft model is completely determined by its aerodynamic derivatives as well as by its inertial and geometric coefficients (which can typically be evaluated experimentally). In this effort, the inertial and geometric characteristics of the WVU YF-22 model were determined with an experimental "swing pendulum" set-up [7]; thus, the remaining critical issue was the determination of the aerodynamic derivatives. Formulas to calculate the entries of the matrices of the linear model in (1) and (2) from the values of the aerodynamic derivatives and geometric-inertial parameters are well known [3]. By inverting such formulas, an initial value for all the main aircraft aerodynamic derivatives was then calculated from the matrices in (1) and (2).

Next, a parameter optimization routine based on routines available within the Matlab Optimization Toolbox® was set up. Specifically, a Matlab routine was written such that it could take as an input the aerodynamic derivatives to be estimated, perform a simulation with the nonlinear model resulting from those derivatives, compare the outputs with the real data, and return the difference (to be minimized) to the caller function. The "fmincon" function – which features the constrained optimization of a multivariable function using a Sequential Quadratic Programming (SQP) technique [8] - was then used to find the set of aerodynamic derivatives providing the best fit with the flight data, starting from the initial set of aerodynamics derivatives calculated from the linear models. The

importance of starting the minimization from a set of already accurate derivatives should be emphasized; in fact, this last optimization can be considered a refinement of the parameters. A lesson learned was that in order for such an optimization to avoid local minima and converge successfully, care must be taken in the selection of the cost function. Specifically, the selected cost function contained 3 terms, a term expressing the RMS of the deviation between real and predicted output, a frequency based term expressing the lowest spectral components of the deviation, and, finally, a term expressing the difference between the current linearized model (obtained by performing a numerical linearization algorithm on the current nonlinear model) and the base linear model in equations (1) and (2).

A final validation of the nonlinear model was then conducted using the validation flight data set, similarly to what was done for the linear model. As shown in Figure 2, the agreement between simulated and real data is substantial.
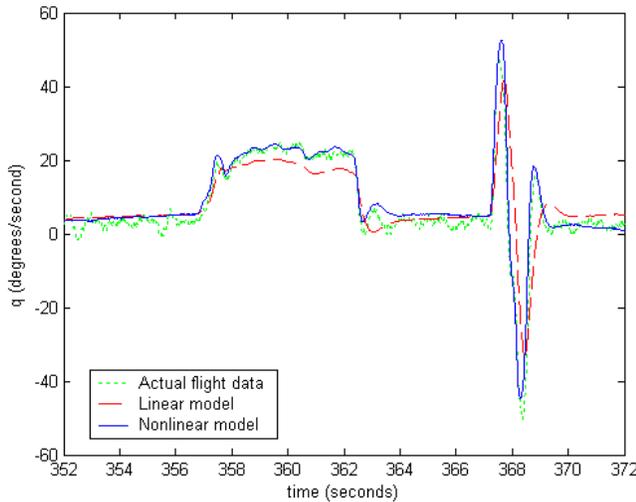

Figure 2 – Linear and nonlinear model prediction versus real flight data

The resulting aircraft nonlinear model is given by:

Geometric and Inertial Data (60% fuel load):
$\overline{c}$ = 0.765 m, b = 1.962 m, S= 1.368 m^2, I_{xx} = 1.607 Kg m^2, I_{yy} = 7.508 Kg m^2, I_{zz} = 7.186 Kg m^2, Ixz = -0.244 Kg m^2, mass = 20.638 Kg, T (engine thrust force) = 54.617 N
Longitudinal Aerodynamic derivatives:
C_{D0} = 0.008, $C_{D\alpha}$ = 0.507, C_{Dq} = 0, $C_{D\delta E}$ = -0.033, C_{L0} = -0.049, $C_{L\alpha}$ = 3.258, C_{Lq} = 0, $C_{L\delta E}$ = 0.189, C_{m0} = 0.022, $C_{m\alpha}$ = -0.473, C_{mq} = -3.449, $C_{m\delta E}$ = -0.364.
Lateral-Directional Aerodynamic derivatives:
C_{Y0} = 0.016, C_{Yb} = 0.272, C_{Yp} = 1.215, C_{Yr} = -1.161, $C_{Y\delta A}$ = 0.183, $C_{Y\delta R}$ = -0.459, C_{l0} = -0.001, C_{lb} = -0.038, C_{lp} = -0.213, C_{lr} = 0.114, $C_{l\delta A}$ = -0.056, $C_{l\delta R}$ = 0.014, C_{n0} = 0, C_{nb} = 0.036, C_{np} = -0.151, C_{nr} = -0.195, $C_{n\delta A}$ = -0.035, $C_{n\delta R}$ = -0.055.

2.3 Actuators and Engine Model Identification

Both signals to the actuators and deflection were measured and recorded. The actuator model was then identified by simple Batch Least Squares (BLS) technique:

$$G_{ACTUATOR}(s) = \frac{23}{s + 23} \qquad (6)$$

Similarly, and both throttle signal and force (a force measuring device was appositely designed and built) were measured and recorded. As for the actuator case, a simple Batch Least Squares (BLS) technique was used to identify a simple engine model containing a time delay, where δ_T is the throttle command and T is the thrust force:

$$\frac{T(s) - T_b(s)}{\delta_T(s)} = \frac{K_T}{(1 + \tau_T s)} e^{-\tau_d s} \qquad (7)$$

where $T_b = -25.86N$, $K_T = 0.624$, $\tau_T = 0.25s$, $\tau_d = 0.26s$

For control synthesis purposes the relationship between throttle command and thrust force can be approximated by a much simpler static affine formula:

$$T = T_b + K_T \delta_T \qquad (8)$$

where δ_T is a digital command between 70 and 255.

3 Formation Geometry

Since flight paths mostly lie on a horizontal plane, (and since gravitational force is perpendicular to such plane), a formation flight control problem can be naturally decomposed into two (almost) independent problems: horizontal (planar) tracking and a vertical tracking.
Note that position and velocity of both leader and follower are expressed with respect to a pre-defined earth-fixed reference frame and are measured by the on-board GPSs.

3.1 Horizontal geometry

The pre-defined formation geometric parameters are the forward clearance f_c and lateral clearance l_c. (Figure 3) The forward distance error f and lateral distance error l can be calculated from positions and velocities using the following formulas:

$$\begin{bmatrix} l \\ f \end{bmatrix} = \begin{bmatrix} \sin(\chi_L) & -\cos(\chi_L) \\ \cos(\chi_L) & \sin(\chi_L) \end{bmatrix} \begin{bmatrix} x_L - x \\ y_L - y \end{bmatrix} - \begin{bmatrix} l_c \\ f_c \end{bmatrix} \qquad (9)$$

where χ_L is the azimuth angle for the leader:

$$\cos(\chi_L) = \frac{V_{Lx}}{\sqrt{V_{Lx}^2 + V_{Ly}^2}}, \text{ and } \sin(\chi_L) = \frac{V_{Ly}}{\sqrt{V_{Lx}^2 + V_{Ly}^2}} \qquad (10)$$

Note that the 2 by 2 matrix in (9) is simply a rotation matrix that rotates the error from an earth fixed reference frame to a reference frame oriented as the velocity of the leader.

3.2 Vertical geometry

The vertical distance error h, can be simply obtained as:
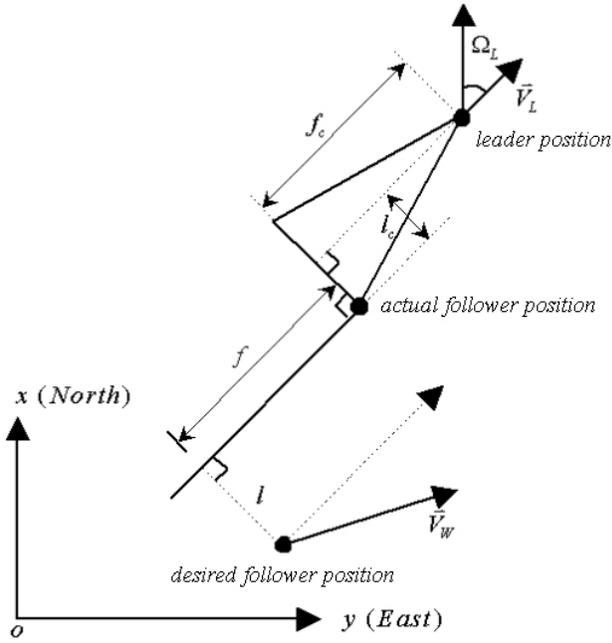$$h = z_L - z - h_c \qquad (11)$$

Figure 3 – Horizontal formation geometry

4 Controller Structure

The whole formation control problem is ultimately a nonlinear control problem in which the controller has to act on throttle and elevator commands to minimize the three errors l, f, and h. It is however useful to note that this problem, like other conventional flight trajectory control problems, exhibits a two-time-scale feature because the trajectory dynamics (relative position and velocity) is slower than the attitude dynamics (angular velocity and orientation). This is why usually both lateral-directional and vertical controllers consist of an inner loop controller (pitch and roll angle tracking) and outer loop controller (lateral-directional and height tracking).

4.1 Outer loop controller

The outer loop controller consists of two parts.
The "vertical" part is a simple linear altitude control. It takes the vertical error (and its derivative) as inputs. The outputs is the desired pitch angle (theta):

$$\theta_d = K_z h + K_{zs}\dot{h} \qquad (12)$$

This desired pitch angle is then taken as a reference signal by the inner loop controller.
The "horizontal" part is a nonlinear dynamic inversion (NLDI) based controller that takes lateral and forward errors (and their derivatives) as inputs. The outputs are the throttle and the desired roll angle (phi).

$$\begin{bmatrix} \delta_T \\ \phi_d \end{bmatrix} = f(\chi - \chi_L, \begin{bmatrix} f \\ l \end{bmatrix}, \begin{bmatrix} \dot{f} \\ \dot{l} \end{bmatrix}) \qquad (13)$$

The desired roll angle is taken as a reference signal by the inner loop controller; the throttle is instead directly used as a control command.

4.2 NLDI Outer Loop horizontal controller: design

This control technique aims at canceling the nonlinearities in the plant dynamics using (output) feedback linearization [9]. In other words, a static nonlinear feedback reduces the system to a series of integrators that can be then controlled by simple linear techniques. In our case, the nonlinear system is the one that has the forward and lateral distance errors f and l as outputs, the desired bank angle ϕ_d and the throttle command δ_T as inputs, and all the states that belong to the lateral dynamics of the follower as states.

According to the feedback linearization technique, we must derive the outputs until the inputs explicitly appear in the expression, and then try to invert the relationship among inputs and derivatives of the outputs. For this problem, the second derivatives of the output are:

$$\begin{bmatrix} \ddot{\ell} \\ \ddot{f} \end{bmatrix} = \begin{bmatrix} V_{xy}\cos(\chi-\chi_L) & \dfrac{V_{xy}}{V}\omega_1\sin(\chi-\chi_L) \\ V_{xy}\sin(\chi-\chi_L) & -\dfrac{V_{xy}}{V}\omega_1\cos(\chi-\chi_L) \end{bmatrix} \begin{bmatrix} \dfrac{g}{V}\tan(\phi_d) \\ T_b + K_T\delta_T \end{bmatrix}$$
$$+ \dfrac{V_{xy}}{V}\omega_2 \begin{bmatrix} -\sin(\chi-\chi_L) \\ \cos(\chi-\chi_L) \end{bmatrix} - \Omega_L V_{xy} \begin{bmatrix} \cos(\chi-\chi_L) \\ \sin(\chi-\chi_L) \end{bmatrix} + \dot{\Omega}_L \begin{bmatrix} f \\ -\ell \end{bmatrix}$$
$$+ \Omega_L \begin{bmatrix} \dot{f} \\ -\dot{\ell} \end{bmatrix} \qquad (14)$$

where:

$$\omega_1 = \frac{1}{m}\cos\alpha\cos\beta ,$$

$$\omega_2 = \frac{\overline{q}S}{m}(C_D\cos\beta - C_Y\sin\beta) + g\sin\gamma \qquad \text{and the}$$

coordinated turn condition is assumed for both leader and wingman:

$$\Omega = \dot{\chi} \cong \dot{\psi} \cong \frac{g}{V}\tan\phi \qquad (15)$$

In practice the coordinated turn condition (15), is imposed by trying to keep both a constant altitude and a zero sideslip angle ($\beta\cong0$) during the turn. In the following, the simplifying assumptions $\alpha=\alpha_0$, $\beta=0$, and $\Omega_L=constant$ have also been made (quasi steady state turn).

Note that both ϕ_d and δ_T appear as inputs in (14) and the 2 x 2 matrix that relates inputs and second derivatives of the output is invertible. Therefore, by inverting Eq. (14), and then replacing $\ddot{f}$ and $\ddot{\ell}$ respectively with $\ddot{f}_d$ and $\ddot{\ell}_d$, (which are the *desired* values for the double derivatives of f and l) we have the following laws.

- Lateral NLDI Control Law:

$$\phi_d = \arctan\left\{\frac{1}{g\cos\gamma}\left[\ddot{\ell}_d\cos(\chi-\chi_L) + \ddot{f}_d\sin(\chi-\chi_L)\right]\right.$$
$$\left. + \frac{V}{g}\Omega_L + \left[\dot{\ell}\sin(\chi-\chi_L) - \dot{f}\cos(\chi-\chi_L)\right]\frac{\Omega_L}{g\cos\gamma}\right\}$$

$$(16)$$

- Forward NLDI Control Law:

$$\delta_T = \frac{m}{K_T\cos\gamma}\left[\ddot{\ell}_d\sin(\chi-\chi_L) - \ddot{f}_d\cos(\chi-\chi_L)\right]$$
$$+ \frac{1}{K_T}\left(\frac{1}{2}\rho_0 V^2 S\left(C_{D0} + C_{D\alpha}\alpha_0\right) + m\sin\gamma - T_b\right)$$
$$- \frac{m}{K_T\cos\gamma}\Omega_L\left[\dot{\ell}\cos(\chi-\chi_L) + \dot{f}\sin(\chi-\chi_L)\right]$$

$$(17)$$

Applying the inputs ϕ_d and δ_T in (17) and (18) to the system in (14) completely cancels the nonlinearities, yielding:

$$\begin{bmatrix}\ddot{\ell}\\\ddot{f}\end{bmatrix} = \begin{bmatrix}\ddot{\ell}_d\\\ddot{f}_d\end{bmatrix}$$

$$(18)$$

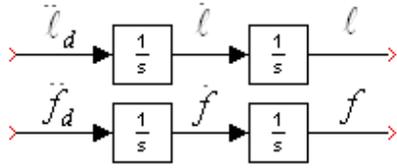that is a linear system consisting of two channels each containing two integrators in series:

Figure 4 – Feedback linearized system

The above system can be easily controlled by a standard linear control, in our case, the chosen controller was:

$$\ddot{\ell}_d = -\tilde{K}_{\ell s}\dot{\ell} - \tilde{K}_\ell\ell$$
$$\ddot{f}_d = -\tilde{K}_{fs}\dot{f} - \tilde{K}_f f$$

$$(19)$$

where the gains were selected so that the controller could be locally equivalent to a previous designed linear one [10]:

$$\tilde{K}_\ell = 0.2027, \quad \tilde{K}_{\ell s} = 0.8894$$
$$\tilde{K}_f = 0.2419, \quad \tilde{K}_{fs} = 2.0560$$
$$K_z = 3.2254, \quad K_{zs} = 1.7593$$

$$(20)$$

4.3 Inner Loop Lateral Controller

The lateral inner loop controller is a simple linear controller that tracks the desired bank angle (supplied by the outer loop controller) and augments the lateral-directional stability of the aircraft:

$$\delta_A = K_p p + K_\phi(\phi - \phi_d)$$

$$(21)$$

$$\delta_R = K_r r$$

$$(22)$$

Classic root-locus based compensation design tools can then be applied to the model for evaluating the controller gains [3]. The basic design specification is to assign the damping ratio of the dominant poles a value around 0.7. The resulting values for the parameters are:

$$K_p = 0.04, \quad K_\phi = 0.35, \quad K_r = 0.16$$

$$(23)$$

4.4 Inner loop Longitudinal Controller

The longitudinal inner loop controller is a simple linear controller that tracks the desired pitch angle (supplied by the outer loop controller):

$$\delta_E = K_q q + K_\theta(\theta - \theta_d)$$

$$(24)$$

The parameters of the controller were calculated using a root locus-based approach [3]:

$$K_q = 0.12, \quad K_\theta = 0.50$$

$$(25)$$

5   Simulation Environment

A Simulink scheme featuring the models of the WVU YF-22 aircraft and the formation controller was developed and implemented.   Given the multi-object nature of the problem, the use of a fully integrated visualization environment was highly desirable. The Virtual Reality Toolbox was used because it allowed for objects and events of a virtual world (coded in VRML 2.0 or higher [11]) to be driven by signals from Matlab/Simulink
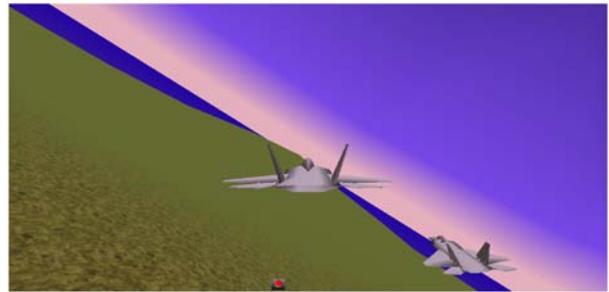

Figure 5 – VRT visualization (behind wingman)

Several simulation studies were conducted to evaluate, test, and optimize several controller and flight configuration parameters. The fact that the controller was coded in Simulink, (using C s-functions) allowed for it to be easily compiled with Real Time Workshop to generate an executable to be uploaded to the flight computer.

6   Flight Test Results

The overall scenario of the formation fight testing experiments is a "leader/follower" combination.   After each aircraft reaches a nominal fight condition, the follower pilot can then engage the autonomous formation controller. The planned flight test was for 2 aircraft to complete several circular pattern laps with the formation controller engaged.   For this particular flight test, the follower had to track the leader trajectory with a preset distance of 30 m forward, 30 m lateral, and 20 m vertical.

Figure 6 shows a captured video image from the ground camera.

Figure 6. Screen shot from ground video

For clarity purposes, only the first lap is shown in the following figures. These plots also feature a simulated follower aircraft, which was set to follow the position of the real leader starting from the same initial condition as the real follower.
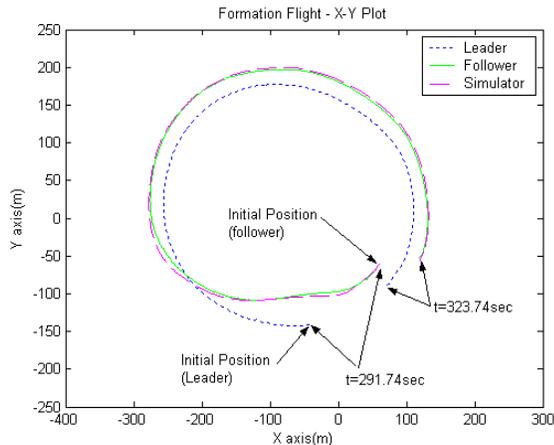

Figure 7. Formation Flight: XY plot

Figure 7 shows the vehicle trajectories in the XY (horizontal) plane. Figure 8 shows the same trajectory within a 3D plot.
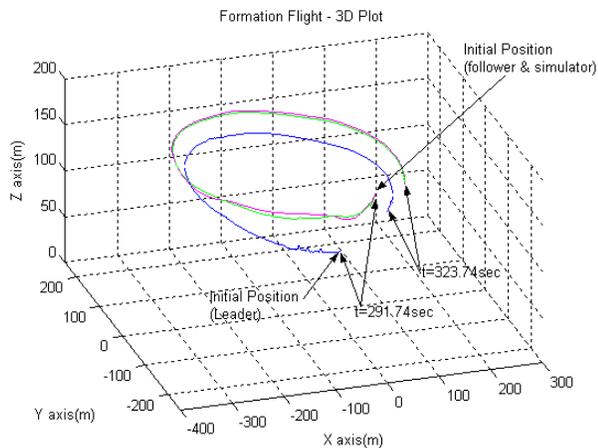

Figure 8. Formation Flight: 3D plot

The above plots show a satisfactory tracking. They also show that the track of the simulated follower remains remarkably close to the track generated by the real follower.

Conclusions

This paper presents a formation flight project that used YF-22 research aircraft developed and built at West Virginia University. Particular emphasis is placed on the design of control laws to maintain the formation of aircraft. The resulting controller has an inner-outer loop structure in which the horizontal outer loop guidance laws rely on feedback linearization. The inner loop controllers are instead linear, and were designed using classical root locus methods. Results of the formation flight test in June 2004 validated the overall design of the formation controller.

Acknowledgement

References

1 – Proud A.W. "Close Formation Flight Control", MS Thesis, AFIT/GE/ENG/99M-24, School of Engineering, Air Force Institute of technology (AU), Wright-Patterson AFB, OH, March 1999

2 - Giulietti F., Pollini L., Innocenti M. , "Formation Flight control: A Behavioral Approach," AIAA GNC Conference 2001, AIAA Paper 2001-4239, Montreal, Canada.

3 - Stevens, B. and Lewis, F. "Aircraft Control and Simulation," John Wiley & Sons, NY, 1992.

4 - Rauw, M.O.: "*FDC 1.2 - A Simulink Toolbox for Flight Dynamics and Control Analysis*". Zeist, The Netherlands, 1997. ISBN: 90-807177-1-1, (http://www.dutchroll.com/)

5 - Ljung, L.,: *System Identification: Theory for the User, 2nd Ed.*, PTR Prentice Hall, Upper Saddle River, Englewood Cliffs, NJ, 1999.

6 - Maine, R.E., Iliff, K.W., "Identification of Dynamic Systems: Theory and Formulation", NASA RF 1168, June 1986

7 - Soule, H. A., Miller, M. P., "The experimental determination of the moments of inertia of airplanes", (http://naca.larc.nasa.gov/reports/1934/). NACA Report 467, 1934

8 - Hock, W. and K. Schittowski, "A Comparative Performance Evaluation of 27 Nonlinear Programming Codes," *Computing*, Vol. 30, p. 335, 1983.

9 - Isidori, A., "*Nonlinear Control Systems*", Springer-Verlag, London, Third edition, 1995.

10 – Campa, G, Napolitano, M. R., Seanor, B, Perhinschi, M. G. "Design of Control Laws For Maneuvered Formation Flight", American Control Conference 2004.

11 - The VRML Web Repository, Dec. 2002: (http://www.web3d.org/x3d/vrml/)